Clinical and Experimental Medicine

Spatial distribution of mast cells around glands in human gastric carcinoma

--Manuscript Draft--

Manuscript Number:	CLEM-D-16-00330R1
Full Title:	Spatial distribution of mast cells around glands in human gastric carcinoma
Article Type:	Original Article
Keywords:	Angiogenesis, chymase, gastric cancer, mast cells, spatial distribution.
Corresponding Author:	Domenico Ribatti, MD University of Bari Medical School Bari, ITALY
Corresponding Author Secondary Information:	
Corresponding Author's Institution:	University of Bari Medical School
Corresponding Author's Secondary Institution:	
First Author:	Diego GUIDOLIN
First Author Secondary Information:	
Order of Authors:	Diego GUIDOLIN
	Simona RUGGIERI
	Tiziana ANNESE
	Cinzia TORTORELLA
	Andrea MARZULLO
	Domenico Ribatti, MD
Order of Authors Secondary Information:	
Funding Information:	“Associazione Italiana Mastocitosi”. Dr. Domenico Ribatti
Abstract:	Angiogenesis, chymase, gastric cancer, mast cells, spatial distribution.
Response to Reviewers:	In reply to Reviewer #1: 1) In the sections analyzed are other cells located nearby MCs and vessels? if so, these additional cells can exert an effect on the different phenotype of mast cells? There are no other inflammatory cells in perivascular position. This location is typical of mast cells. 2) Are these MC stained for other pro-angiogenic mediators such as VEGF? In this case, any differences were observed in mast cells expressing VEGF between grade IV and grade II? We don’t’ have stained the section with an anti-VEGF antibody. Nevertheless, other Authors have previously investigated this aspect and have demonstrated an higher VEGF expression in grade IV specimens as compared to grade II ones (References 4 and 9 of the Reference List and Nam et al., Cancer Res Treat 2002;34:41-5). 3) For sake of completeness, I would suggest that the Authors add the following reference. Puxeddu I, Piliponsky AM, Bachelet I, Levi-Schaffer F. Mast cells in allergy and beyond. Int J Biochem Cell Biol. 2003 Dec;35(12):1601-7. Review. We have added this reference. In reply to Reviewer #2

	English must be corrected, some spelling problems may be resolved. The Ms has been revised by an English native speaker. Lack of significant correlation is given by low number of cases but this fact does not affect the valuabe methods which must be extensively used for the quantification of interrelation between mast cells, tumor blood vessels and tumor cells. As suggested also by the Reviewer, the low number of patients is justified by the complexity of the methods used to estimate the spatial distribution of the mast cells.
Suggested Reviewers:	Anca M. CIMPEAN Univerity of Timisoara Medical School, ROMANIA anca.cimpean1972@yahoo.com She is an expert in this field.
	Valentin DJONOV University of Berne Medical School, SWITZERLAND valentin.djonov@ana.unibe.ch He is an expert in this field
	Sandra LIEKENS University of Lovanio Medical School, BELGIUM sandra.liekens@rega.kuleuven.be She is an expert in this field

MS CLEM-D-16-00330-REVISED

Spatial distribution of mast cells around vessels and glands in human gastric carcinoma

Running head: Mast cells in gatric carcinoma

Diego Guidolin [a], Simona Ruggieri [b], Tiziana Annese [b], Cinzia Tortorella [a], Andrea Marzullo [c], Domenico Ribatti [b, d]

[a] Department of Molecular Medicine, University of Padova Medical School, University of Padova, Italy.

[b] Department of Basic Medical Sciences, Neurosciences, and Sensory Organs, University of Bari Medical School, Bari, Italy

[c] Department of Emergency and Transplantation, Pathology Section, University of Bari Medical School, Bari, Italy

[d]National Cancer Institute "Giovanni Paolo II", Bari, Italy

Correspondence to:

Prof. Domenico RIBATTI

Department of Basic Medical Sciences, Neurosciences, and Sensory Organs

University of Bari Medical School

Piazza Giulio Cesare, 11

70124 Bari, Italy

Phone: +39.080.5478326

Fax: +39.080.5478310

E mail: domenico.ribatti@uniba.it

Abstract.

The spatial distribution of mast cells inside the tumor stroma has been little investigated. In this study, we have evaluated tumor mast cells (MCs) distribution in gastric cancer through the analysis of the morphological features of the spatial patterns generated by these cells, including size, shape, and architecture of the cell pattern. The pattern of distribution of tryptase- and chymase-positive MCs around the blood vessels and gastric glands in human gastric adenocarcinoma samples was investigated by immunohistochemical techniques and by introducing a quantitative approach to characterize the spatial distribution of MCs .In human gastric cancer both chymase-positive MC and vessels exhibited significant deviations from randomness for what it concerns their spatial relationship with gastric parenchyma. As indicated by cell-to-gland distances shorter than expected by chance, in grade II samples a preferential localization of chymase-positive MC near the gastric glands was observed. Interestingly, the same type of spatial association was exhibited by vessels in grade IV samples, where vessel-to-gland distances shorter than expected by chance were observed. These two findings allow to speculate about a sequence of events in which a subpopulation of MC is first recruited around gastric parenchyma to drive the subsequent development of a vascular support to the tissue.

Key Words. Angiogenesis, chymase, gastric glands, gastric cancer, mast cells, spatial distribution; vessels.

1. Introduction

Increased vascularity is associated with haematogenous and lymph node metastasis and poor prognosis of gastric cancer [1-7].Vascular endothelial growth factor (VEGF), fibroblast growth factor-2 (FGF-2), and platelet derived endothelial cell growth factor (PD-ECGF) expression correlate with tumor stage [8, 9, 4]. Moreover, VEGF receptors 1 and 2 (VEGFR-1 and VEGFR-2) are expressed in gastric cancer and their overexpression is associated with angiogenesis and metastases to distant organs [10, 11].

Mast cells (MCs) accumulate in the stroma surrounding tumors, where they secrete angiogenic cytokines and proteases [12]. We have previously demonstrated that MC density correlates with angiogenesis and progression of patients with gastric carcinoma [13]. More recently, Ammendola et al. [14] have shown that tryptase-positive MCs and c-kit receptor expressing cells correlate with angiogenesis and lymph node metastasis in gastric cancer.

The aim of this study was to further contribute to the knowledge of tumor MC distribution, investigating the pattern of distribution of tryptase- and chymase-positive MCs around the blood vessels and gastric glands in human gastric adenocarcinoma samples by introducing a quantitative approach to characterize their spatial distribution.

2. Materials and Methods

2.1. Bioptic specimens. Specimens of primary gastric adenocarcinomas were obtained from 17 patients who had undergone curative gastrectomy. None of these patients received preoperative treatment such as radiation and chemotherapy.

According to histological stage, eight had stage II disease, and nine had stage IV disease. Tissue samples were fixed in formalin and embedded in paraffin according to standard procedures. Four µm-thick sections were cut and mounted on glass slides. Full ethical approval and signed informed consent from individual patients were obtained to conduct the study. All procedures followed were in accordance with the ethical standards of the responsible committee on human experimentation (institutional and national) and with the Helsinki Declaration of 1964 and later versions.

2.2. Immunohistochemistry . Three murine monoclonal antibodies (MAb) against the endothelial cell marker CD31 (MAb 1A10; Dako, Glostrup, Denmark) and against MC markers tryptase and chymase (Mab AA1, Dako, and, respectively, MabCC1, Novocastra Laboratories Ltd, Newcastle, UK) were used in this study. Briefly, sections were collected on 3-amino-propyltriethoxysilane coated slides, deparaffinized by the xylene ethanol sequence, rehydrated in a graded ethanol scale and in Tris-buffered saline (TBS, pH 7.6) and incubated overnight at 4°C with the MAbs (1:25 in TBS), after prior antigen retrieval by enzymatic digestion with Ficin (Sigma, St Louis, MO, USA) for 30 min at room temperature. The immunodetection was performed with alkaline phosphatase anti-alkaline phosphatase (APAAP, Dako) and Fast Red as chromogen, followed by haematoxylin counterstaining. A preimmune serum (Dako) replacing the primary antibody served as negative control.

2.3. Image analysis methods. Computer-assisted image analysis was performed to evaluate the area density of CD31-, tryptase- and chymase-positive regions in the tissue samples. The image analysis system included a light microscope (DM-R; Leica Microsystems, Wetzlar, Germany) and a high-resolution digital camera (DC200; Leica Microsystems) transmitting image data to a PC equipped with appropriate

software for image acquisition and analysis (QWin; Leica Microsystems, Cambridge, UK). The images of four 200 x magnifications random fields for each of three sections per sample were then acquired, processed to correct shading and enhance the contrast and stored as TIFF files. Images were analyzed according to a previously detailed procedure [15]. Briefly, specifically immunostained structures were identified by selecting the pixels with color hue in a specified yellow orange range (to exclude all the blue haematoxylin stained nuclei) and brightness lower than the mean brightness level exhibited by the negative control sections minus three standard deviations (thus excluding the unspecific staining). The total area of the identified structures was then measured and expressed as percentage of the total area of the analyzed field.

Computer-assisted image analysis was performed also to characterize the distribution of MCs around vessels and gland profiles. At a primary magnification of 20 x five randomly chosen fields per section were selected and their images acquired in full colors (RGB, 24-bit), processed to correct shading, then filed TIFF. All the image analysis procedures were performed by using the ImageJ software , freely available at http://rsb.info.nih.gov/ij/. Color deconvolution was first applied to allow the identification of immunopositive structures. This procedure implements stain separation according to the method by Ruifrok and Johnston [16] and was performed by using an ImageJ plugin specifically developed by Gabriel Landini (see http://www.mecourse.com/landinig/software/software.html). As shown in Fig 1A, this procedure leads to the generation of two images containing haematoxylin- and DAB-stained structures respectively. From the latter one, immunopositive profiles can then be easily discriminated by conventional thresholding methods and the total amount of immunoreactivity was evaluated by estimating the percent of periglandular tissue area

(Area%) occupied by positive structures. When applied to the images from tryptase- or chymase-stained sections this procedure also allows a direct discrimination of MC profiles and the evaluation of their positions (i.e. x, y-coordinates of the gravity centers). As far as CD31-positive patterns are concerned, a reliable discrimination of single vessel profiles cannot be achieved. Thus, the abovementioned analysis was applied to a sub sample binary image of the cell patterns (Fig. 1 B). The sub sampling was obtained by extracting from the binary image of each pattern the set of pixels corresponding to the points of a superimposed regular grid [17]. The x, y-coordinates of the gravity centers of the selected points were then recorded. Further processing of the obtained data was then applied to characterize the following morphological features of the tissue samples:

2.4. Distances between MC or vessels and gastric glands. To estimate the distance of each MC profile from the glands, a binary image of the glands was obtained by interactively tracing their profiles and further processed to calculate its 'distance transform' [18]. This algorithm provides a map where each background pixel is labelled (Fig. 2) with a value equal to its distance from the nearest pixel belonging to a gland profile. The distance from glands of each cell profile was then evaluated by the value the map exhibited at the location corresponding to the x, y-coordinates of the cell profile. Around the observed set of gland profiles, 10 random (Poisson) point patterns were finally computer generated. Each pattern had a number of points equal to the number of observed MC profiles. They underwent the previously described analysis in order to provide Monte Carlo estimates [19] of the distances from vessels in the case of complete spatial randomness (CSR). The same procedure was also

applied to the representative points of CD31-positive patterns to estimate distances between vessels and glands.

2.5. Architecture of the MC or vessel patterns. To describe the spatial distribution of the MC within the cell pattern a uniformity index (UI) was estimated according to a previously described procedure [17], schematically illustrated in Fig. 3. The same procedure was also applied to the representative points of CD31-positive patterns to evaluate their overall architecture. UI can assume any value between 1 (when the objects are distributed in a regular array) and 0 (when maximal clustering occurs). The value the parameter assumes when a random (Poisson) spatial distribution of profiles occurs was estimated on the abovementioned computer generated random patterns.

2.6. Statistics. Samples were grouped according to the applied staining and within each sample Area% and UI values were averaged to provide representative values for that sample. Differences between grade II and grade IV groups were then tested by unpaired Student's t-test. Paired Student's t-test was instead applied to statistically identify differences between the observed UI values and those estimated on the corresponding computer generated random point patterns. The GraphPad Prism 3.0 statistical package (GraphPad Software Inc., San Diego CA, USA) was used for the analysis and $p \leq 0.05$ was considered as the limit for statistical significance. For each group, the cumulative frequency distribution [G(d)] of all the observed profile-to-gland distances was calculated. Its expected value under CSR [$G_0(d)$] was estimated by averaging the cumulative frequency distributions of the distances from glands obtained from the 10 simulated random point patterns. To interpret the profile-to-

gland spatial relationship statistically, the 95% confidence envelope for $G_0(d)$ was also calculated from the Monte Carlo simulations [20]. The null hypothesis is that there is no difference between the two functions, i.e. $G(d) = G_0(d)$ for all d. Thus, if G(d) is greater than the confidence envelope around $G_0(d)$, then the profiles are clustered around the glands, i.e. they are closer to the glands than expected by chance. If G(d) is lower than the envelope around $G_0(d)$, then short profile-to-gland distances are less frequent than expected by chance, i.e. the placement of the investigated structures close to the glands was 'inhibited' [21].

3. Results

CD31-positive blood vessels and tryptase- and chymase-positive MCs are more numerous in bioptic specimens of stage IV gastric cancer as compared with stage II (Fig. 4). Moreover, the number of chymase-positive was significantly lower than the number of tryptase-positive MCs. This morphological observation was confirmed by morphometric evaluation, as shown in Fig. 5. The percent area covered by CD31-positive structures or by MCs was significantly higher in the grade IV group than in the grade II samples. Despite the significant differences in size of the CD31-, chymase- and tryptase-positive patterns in the two analyzed conditions, no significant differences were detected between grade II and grade IV samples in the parameter UI (Fig. 6) describing the spatial relationships between the elements forming each pattern. Moreover, no significant difference was identified when the experimental patterns were compared to the corresponding computer-generated random point patterns, suggesting for vessels and MC populations a spatial architecture consistent with a random spatial distribution of the elements within the pattern. As far as the

spatial relationship between MC or vessels and gastric glands was considered, no significant spatial association between tryptase-positive cells and glands was observed in both grade II and grade IV groups. However, as shown in Fig. 7, in grade II samples chymase-positive cells appeared clumped around gastric glands as indicated by an amount of short cell-to-gland distances significantly higher than expected under complete spatial randomness, while CD31-positive structures didn't show any significant spatial association with gastric glands. In grade IV samples, on the contrary, vessels appeared significantly associated with gastric glands, being preferentially located at distances of about 35-50 μm with a frequency significantly higher than expected by chance.

4. Discussion

MCs represent a cell population widely distributed in connective tissue and several studies indicate a mutual spatial and functional relationship between MCs and vascular endothelial cells. MCs have been implicated in the regulation of physiological and pathological examples of angiogenesis including wound healing [22], ovulation [23], and chronic inflammation [24]. Of significant interest is the increasing evidence of the involvement of MCs in the angiogenic processes occurring in vascular tumors, like hemangioma and hemangioblastoma [25, 26], as well as in a number of hematological and solid tumors, including lymphomas [27-29], multiple myeloma [30], myelodysplastic syndrome [31], B cell chronic lymphocytic leukemia [32], breast cancer [33, 34], colon-rectal cancer [35], uterine and cervix cancer [36-38], melanoma [39-41], and pulmonary adenocarcinoma [42], in which MC accumulation correlates with increased neovascularization, VEGF and FGF-2 expression, tumor aggressiveness, and poor prognosis [43, 44].

In the present study we have further expanded the investigation by analyzing the spatial distributions of MCs and vessels in gastric cancer, their relationship with gastric parenchyma and the changes they undergo as far as the pathology gets worse. The approach here followed derived from spatial statistics [45, 46] and was based on the statistical analysis of the distribution of the distances of MCs and vessels from gastric glands with the aim to objectively establish whether MCs and vessels displayed any kind of spatial association with gastric parenchyma. Such an analysis involved the comparison of the observed distribution of MC/vessels-to-gland distances with the one corresponding to the case of complete spatial randomness, i.e., in which the analyzed structures are distributed randomly in the stromal compartment. In order to get an insight on possible changes the studied relationship can have as far as the pathology progresses, samples from pathological tissues at different stages of the disease were considered.

The results of the study indicated that in human gastric cancer both chymase-positive MCs and vessels exhibited significant deviations from randomness for what it concerns their spatial relationship with gastric parenchyma. As indicated by cell-to-gland distances shorter than expected by chance, in grade II samples a preferential localization of chymase-positive MCs near the gastric glands was observed. Interestingly, the same type of spatial association was exhibited by vessels in grade IV samples, where vessel-to-gland distances shorter than expected by chance were observed.

These two findings allow to speculate about a sequence of events in which a subpopulation of MC is first recruited around gastric parenchyma to drive the subsequent development of a vascular support to the tissue. Although more specific and direct experimental investigations would be needed, this hypothesis shows

consistency with the well documented relationship between MC and angiogenesis in tumors, where they preferentially accumulate at the periphery of the tumor, within the surrounding connective tissue [47]. The fact that MCs contribute to the induction of tumor angiogenesis has been demonstrated in studies on MC-deficient mice, which display slow angiogenesis and its restoration after local reconstitution of MCs [48]. MCs contain many angiogenic factors and a variety of cytokines [49], such as transforming growth factor-beta, tumor necrosis factor-alpha [50], interleukin-8 [51], FGF-2 [52] and VEGF [53], implicated in normal as well as tumor-associated neo-angiogenesis. Of particular interest for the present discussion are evidences suggesting chymase as a major factor in MC-mediated angiogenesis. In the hamster sponge-implant model it induced formation of granulomas and angiogenesis in a time- and dose-dependent manner [54]. Furthermore, this angiogenic response was inhibited by chymase inhibitors including chymostatin and trypsin inhibitors, but not by a tryptase inhibitor like leupeptin [54]. The angiogenic activity of this protease stored in MC granules was also confirmed *in vivo* in chick embryo chorioallantoic membrane assay [55].

Ethical Approval and Informed Consent. All procedures followed were in accordance with the ethical standards of the responsible committee on human experimentation (institutional and national) and with the Helsinki Declaration of 1964 and later versions. Informed consent was obtained from all patients for being included in the study.

Competing interests. Conflict of interest: None.

Acknowledgement. This work has been supported by the "Associazione Italiana Mastocitosi".

5. References

1. Ammendola M, Sacco R, Donato G, et al. Mast Cell Positivity to Tryptase Correlates with Metastatic Lymph Nodes in Gastrointestinal Cancer Patients Treated Surgically. Oncology. 2013;85:111-6.
2. Araya M, Terashima M, Takagane A, et al. Microvessel count predicts metastasis and prognosis in patients with gastric cancer. J Surg Oncol. 1997;65:232-6.
3. Maeda K, Chung YS, Takatsuka S, et al. Tumour angiogenesis and tumour cell proliferation as prognostic indicators in gastric carcinoma. Brit J Cancer. 1995;72:319-23.
4. Takahashi Y, Cleary KR, Mai M, Kitadai Y, Bucana CD, Ellis LM. Significance of vessel count and vascular endothelial growth factor and its receptor (KDR) in intestinal-type gastric cancer. Clin Cancer Res. 1996;2:1679-84.
5. Tanigawa N, Amaya H, Matsumura M, Shimomatsuya T. Association of tumour vasculature with tumour progression and overall survival of patients with non-early gastric carcinomas. Brit J Cancer. 1997;75:566-71.
6. Tanigawa N, Amaya H, Matsumura M, Shimomatsuya T. Correlation between expression of vascular endothelial growth factor and tumor vascularity, and patient outcome in human gastric carcinoma. J Clin Oncol. 1997;15:826-32.
7. Tanigawa N, Amaya H, Matsumura M, et al. Extent of tumor vascularization correlates with prognosis and hematogenous metastasis in gastric carcinomas. Cancer Res. 1996;56:2671-6.
8. Maeda K, Chung Y-s, Ogawa Y, et al. Prognostic value of vascular endothelial growth factor expression in gastric carcinoma. Cancer. 1996;77:858-63.
9. Takahashi Y, Bucana CD, Akagi Y, et al. Significance of platelet-derived endothelial cell growth factor in the angiogenesis of human gastric cancer. Clin Cancer Res. 1998;4:429-34.
10. Maehara Y, Kabashima A, Koga T, et al. Vascular invasion and potential for tumor angiogenesis and metastasis in gastric carcinoma. Surgery. 2000;128:408-16.
11. Zhang H, Wu J, Meng L, Shou CC. Expression of vascular endothelial growth factor and its receptors KDR and Flt-1 in gastric cancer cells. World J Gastroenterol. 2002;8:994-8.
12. Ribatti D, Crivellato E. Mast Cells and Tumours. Springer Science + Business Media; 2011.
13. Ribatti D, Guidolin D, Marzullo A, et al. Mast cells and angiogenesis in gastric carcinoma. Int J Exp Pathol. 2010;91:350-6.
14. Ammendola M, Sacco R, Sammarco G, et al. Mast Cells Positive to Tryptase and c-Kit Receptor Expressing Cells Correlates with Angiogenesis in Gastric Cancer Patients Surgically Treated. Gastroenterol Res Pract. 2013;2013:1-5.
15. Guidolin D, Zunarelli E, Genedani S, et al. Opposite patterns of age-associated changes in neurons and glial cells of the thalamus of human brain. Neurobiol of Aging. 2008;29:926-36.
16. Ruifrok AC, Katz RL, Johnston DA. Comparison of Quantification of Histochemical Staining By Hue-Saturation-Intensity (HSI) Transformation and Color-Deconvolution. Appl Immunohisto M M. 2003;11:85-91.
17. Guidolin D, Marinaccio C, Tortorella C, et al. A fractal analysis of the spatial distribution of tumoral mast cells in lymph nodes and bone marrow. Exp Cell Res. 2015;339:96-102.

18. R J. The Image Processing Handbook (6th ed.). Boca Raton, FL: Taylor & Francis. 2011.
19. Besag J, Diggle PJ. Simple Monte Carlo Tests for Spatial Pattern. Appl Stat. 1977;26:327.
20. Gatrell AC, Bailey TC, Diggle PJ, Rowlingson BS. Spatial Point Pattern Analysis and Its Application in Geographical Epidemiology. T I Brit Geogr. 1996;21:256.
21. Philimonenko AA, Janáček J, Hozák P. Statistical Evaluation of Colocalization Patterns in Immunogold Labeling Experiments. J Struct Biol. 2000;132:201-10.
22. Trabucchi E, Radaelli E, Marazzi M et al. The role of mast cells in wound healing. Int J Tissue React. 1988;10:367-72.
23. Krishna A, Beesley K, Terranova PF. Histamine, mast cells and ovarian function. J Endocrinol. 1989;120:363-71.
24. Yamada T, Sawatsubashi M, Itoh Y, et al. Localization of vascular endothelial growth factor in synovial membrane mast cells: examination with ”multi-labelling subtraction immunostaining". Virchows Arch. 1998;433:567-70.
25. Glowacki J, Mulliken JB. Mast cells in hemangiomas and vascular malformations. Pediatrics. 1982;70:48-51.
26. Qu Z, Kayton RJ, Ahmadi P, et al. Ultrastructural Immunolocalization of Basic Fibroblast Growth Factor in Mast Cell Secretory Granules: Morphological Evidence for bFGF Release Through Degranulation. J Histochem Cytochem. 1998;46:1119-28.
27. Marinaccio C, Ingravallo G, Gaudio F, et al. Microvascular density, CD68 and tryptase expression in human Diffuse Large B-Cell Lymphoma. Leukemia Res. 2014;38:1374-7.
28. Ribatti D, Nico B, Vacca A, et al. Do mast cells help to induce angiogenesis in B-cell non-Hodgkin's lymphomas? Brit J Cancer. 1998;77:1900-6.
29. Ribatti D, Vacca A, Marzullo A, et al. Angiogenesis and mast cell density with tryptase activity increase simultaneously with pathological progression in B-cell non-Hodgkin's lymphomas. Int J Cancer. 2000;85:171-5.
30. Ribatti D, Vacca A, Nico B, et al. Bone marrow angiogenesis and mast cell density increase simultaneously with progression of human multiple myeloma. Brit J Cancer. 1999;79:451-5.
31. Ribatti D, Polimeno G, Vacca A, et al. Correlation of bone marrow angiogenesis and mast cells with tryptase activity in myelodysplastic syndromes. Leukemia. 2002;16:1680-4.
32. Molica S, Vacca A, Crivellato E, Cuneo A, Ribatti D. Tryptase-positive mast cells predict clinical outcome of patients with early B-cell chronic lymphocytic leukemia. Eur J Haematol. 2003;71:137-9.
33. Bowrey PF, King J, Magarey C, et al. Histamine, mast cells and tumour cell proliferation in breast cancer: does preoperative cimetidine administration have an effect? Br J Cancer. 2000;82:167-70.
34. Hartveit F. Mast cells and metachromasia in human breast cancer: Their occurrence, significance and consequence: A preliminary report. J Pathol. 1981;134:7-11.
35. Lachter J, Stein M, Lichtig C, Eidelman S, Munichor M. Mast cells in colorectal neoplasias and premalignant disorders. Dis Colon Rectum. 1995;38:290-3.
36. Benitez-Bribiesca L, Wong A, Utrera D, Castellanos E. The Role of Mast Cell Tryptase in Neoangiogenesis of Premalignant and Malignant Lesions of the Uterine Cervix. J histochem cytochem. 2001;49:1061-2.

37. Guidolin D, Marinaccio C, Tortorella C, et al. Non-random spatial relationships between mast cells and microvessels in human endometrial carcinoma. Clinical Exp Med. 2016.
38. Ribatti D, Finato N, Crivellato E, et al. Neovascularization and mast cells with tryptase activity increase simultaneously with pathologic progression in human endometrial cancer. Am J Obstet Gynecol. 2005;193:1961-5.
39. Dvorak AM, Mihm MC, Osage JE, Dvorak HF. Melanoma. An Ultrastructural Study of the Host Inflammatory and Vascular Responses. J Invest Dermatol. 1980;75:388-93.
40. Reed JA, McNutt NS, Bogdany JK, Albino AP. Expression of the mast cell growth factor interleukin-3 in melanocytic lesions correlates with an increased number of mast cells in the perilesional stroma: implications for melanoma progression. J Cutan Pathol. 2006;23:495-505.
41. Ribatti D, Vacca A, Ria R, et al. Neovascularisation, expression of fibroblast growth factor-2, and mast cells with tryptase activity increase simultaneously with pathological progression in human malignant melanoma. Eur J Cancer. 2003;39:666-74.
42. Ullah E, Nagi A, Lail R. Angiogenesis and mast cell density in invasive pulmonary adenocarcinoma. J Canc Res Ther. 2012;8:537.
43. Ribatti D, Ennas MG, Vacca A, et al. Tumor vascularity and tryptase-positive mast cells correlate with a poor prognosis in melanoma. Eur J Clin Invest. 2003;33:420-5.
44. Toth-Jakatics R, Jimi S, Takebayashi S, Kawamoto N. Cutaneous malignant melanoma: correlation between neovascularization and peritumor accumulation of mast cells overexpressing vascular endothelial growth factor. Hum Pathol. 2000;31:955-60.
45. Diggle PJ BJ, Gleaves T. Statistical Analysis of Spatial Point Patterns. Academic Press, London. 1976:1983:p. 354.
46. R B. Tests for randomness for spatial point patterns. J R Statist Soc. 1979:B41:368-74.
47. Ribatti D, Finato N, Crivellato E, et al. Angiogenesis and mast cells in human breast cancer sentinel lymph nodes with and without micrometastases. Histopathology. 2007;51:837-42.
48. Starkey JR, Crowle PK, Taubenberger S. Mast-cell-deficient W/Wv mice exhibit A decreased rate of tumor angiogenesis. Int J Cancer. 1988;42:48-52.
49. Puxeddu I, Piliponsky AM, Bachelet I, Levi-Schaffer F. Mast cells in allergy and beyond. Int J Biochem Cell Biol. 2003;35:1601-1607.
50. Norrby K. Oral administration of a nitric oxide synthase inhibitor enhances de novo mammalian angiogenesis mediated by TNF-alpha, saline and mast-cell secretion. Acta Pathol Mic Sc. 2000;108:496-502.
51. Grutzkau A, Kruger-Krasagakes S, Kogel H, Moller A, Lippert U, Henz BM. Detection of Intracellular Interleukin-8 in Human Mast Cells: Flow Cytometry as a Guide for Immunoelectron Microscopy. J histochem cytochem. 1997;45:935-45.
52. Qu Z, Liebler JM, Powers MR, et al. Mast cells are a major source of basic fibroblast growth factor in chronic inflammation and cutaneous hemangioma. Am J Pathol. 1995;147:564-73.
53. Grutzkau A, Kruger-Krasagakes S, Baumeister H, et al. Synthesis, Storage, and Release of Vascular Endothelial Growth Factor/Vascular Permeability Factor

(VEGF/VPF) by Human Mast Cells: Implications for the Biological Significance of VEGF206. Mol Biol Cell. 1998;9:875-84.

54. Muramatsu M, Katada J, Hattori M, Hayashi I, Majima M. Chymase mediates mast cell-induced angiogenesis in hamster sponge granulomas. Eur J Pharmacol. 2000;402:181-91.

55. Ribatti D, Ranieri G, Nico B, Benagiano V, Crivellato E. Tryptase and chymase are angiogenic in vivo in the chorioallantoic membrane assay. Int J Dev Biol. 2011;55:99-102.

Legend to Figures

Figure 1: **A.** Full color image from a sample visualizing a haematoxylin-counterstained CD31-positive pattern (left panel). By applying a color deconvolution procedure (see text), the two stains can be efficiently separated (right panel). **B.** From the DAB stained component the CD31-positive structures can be easily discriminated. They are shown together with the regular grid used to subsample the binary image of the CD31-positive patterns (left panel). The result of the sub sampling procedure (right panel) is a set of representative points to be used for the analysis of the spatial distribution of the pattern (see text).

Figure 2: A. Field image showing tryptase-positive MCs (brown) and gland profiles outlined in yellow. **B.** Distance transform of the image shown in A: periglandular pixels are labeled according to their distance from the nearest gland profile boundary as indicated by the color-coded map. **C.** The locations of the tryptase-positive cell profiles are shown. The distance of each cell profile from the glands can be estimated by the value of the distance map at the point where the cell profile is located (i.e. at its x, y-coordinates). **D.** A random (Poisson) pattern with the same number of points as the cell pattern in **C** computer-generated in the same tissue area (see text).

Figure 3. Schematic illustration of the procedures used to estimate the 'uniformity index' used to describe the architecture of an immunopositive pattern. A tryptase-positive cell pattern is shown in **A**. It contains *N* cells unevenly spaced. Their positions within the periglandular tissue (outlined in blue) are shown in **B**. If they were evenly spaced (regular array of profiles) the distance (*d*) between their gravity centers would be given by the square root of the ratio *Periglandular tissueArea/N*.

Thus, when a dilation of size *(d/2-1)* is applied to the gravity centers of the cells in the uneven pattern in B, some of the points will merge together and the number of objects after dilation will be *N'<N*. They are shown in **C**. The index of uniformity is defined as *UI=N'/N* [15]**..**

Figure 4. Immnohistochemical staining for CD31, tryptase and chymase in stage II (a–c) and stage IV (d–f) human gastric cancer. In (a, d) endothelial cells immunoreactive for CD31; in (b, e) tryptase-positive mast cells; in (c, f) chymase-positive mast cells. Blood vessels and mast cells are distributed around the gastric glands. Original magnification: a–f, x 200.

Figure 5. The amount of periglandular space occupied by CD31-, chymase- and tryptase-positive structures increases from grade II to grade IV gastric cancer. Values are mean ± sem. *p<0.05; **p<0.01 (two-samples Student's t-test).

Figure 6: Uniformity index values (mean ± sem) of the analyzed immunoreactivity pattern in grade II and grade IV samples. The parameter estimates the degree of spatial uniformity of a pattern (see text) increasing from 0 (maximal clustering) to 1 (regular array of elements). The white column shows the mean UI value estimated on the computer-generated random (Poisson) point patterns.

Figure 7. Analysis of the spatial relationship between chymase-positive MCs (upper panel) or microvessels (lower panel) and gastric glands. Solid lines indicate the difference between the observed distribution of structure-to-gland distances [G(d)] and the estimated distribution [G_0(d)] under complete spatial randomness (CSR).

Dotted lines indicate the 95% confidence envelope for CSR. In grade II gastric cancer samples there is a spatial association between chymase-positive MCs and glands as indicated by a frequency of short cell-to-vessel distances significantly higher than expected by chance (grey area). A significant spatial association between microvessels and glands was found in grade IV samples.

Figure 1

Click here to download Figure Fig1.jpg

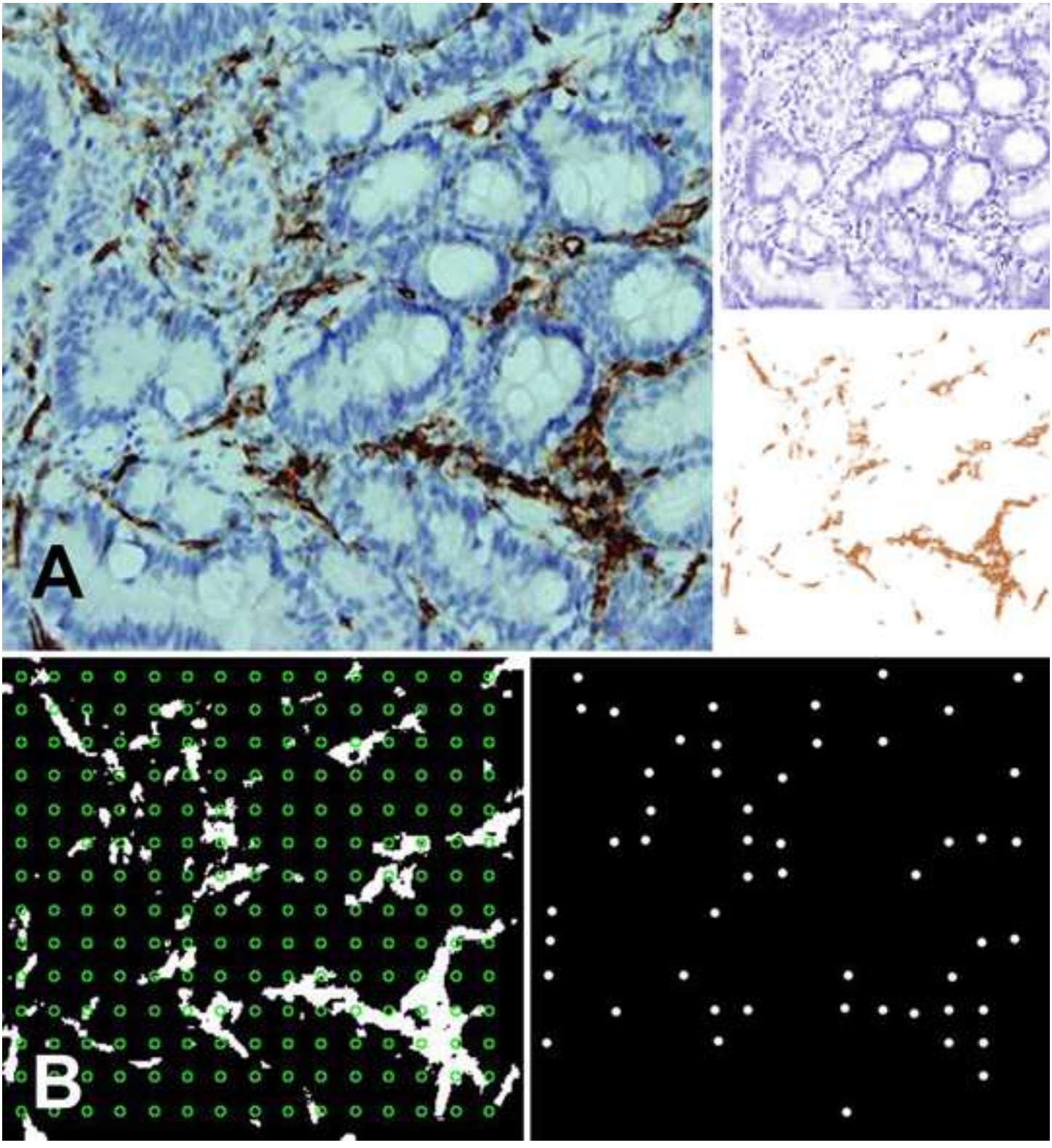

Figure 3

Click here to download Figure Fig2.jpg

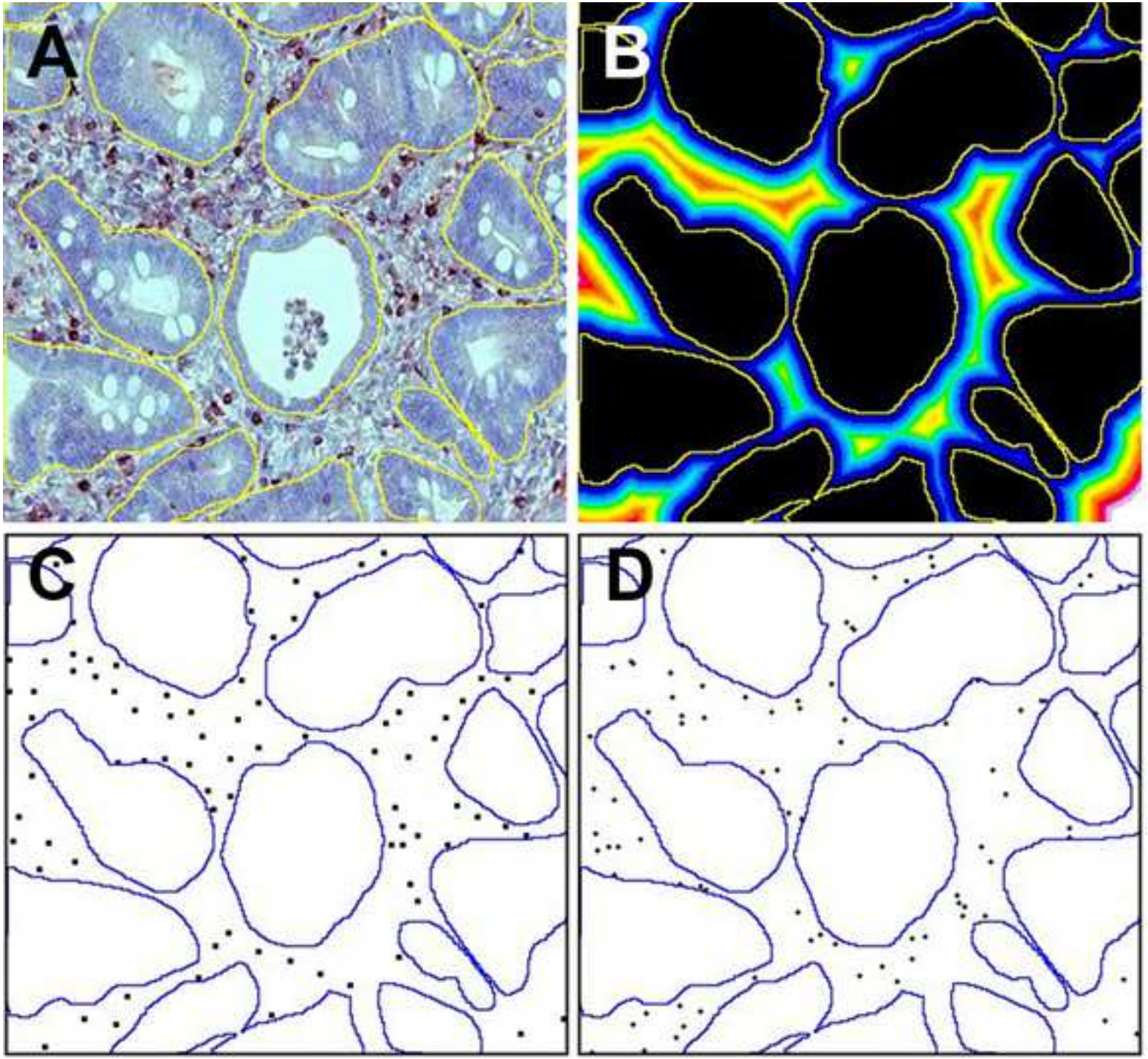

Figure 3

Click here to download Figure Fig3.jpg

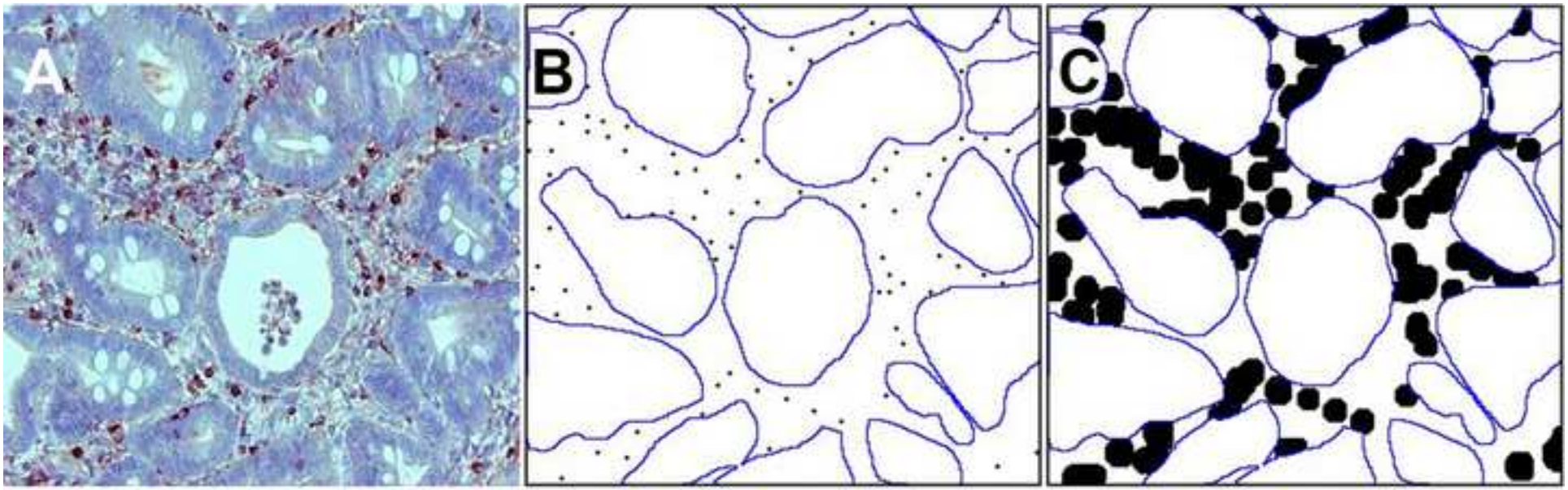

Figure 4

Click here to download Figure Fig4.jpg

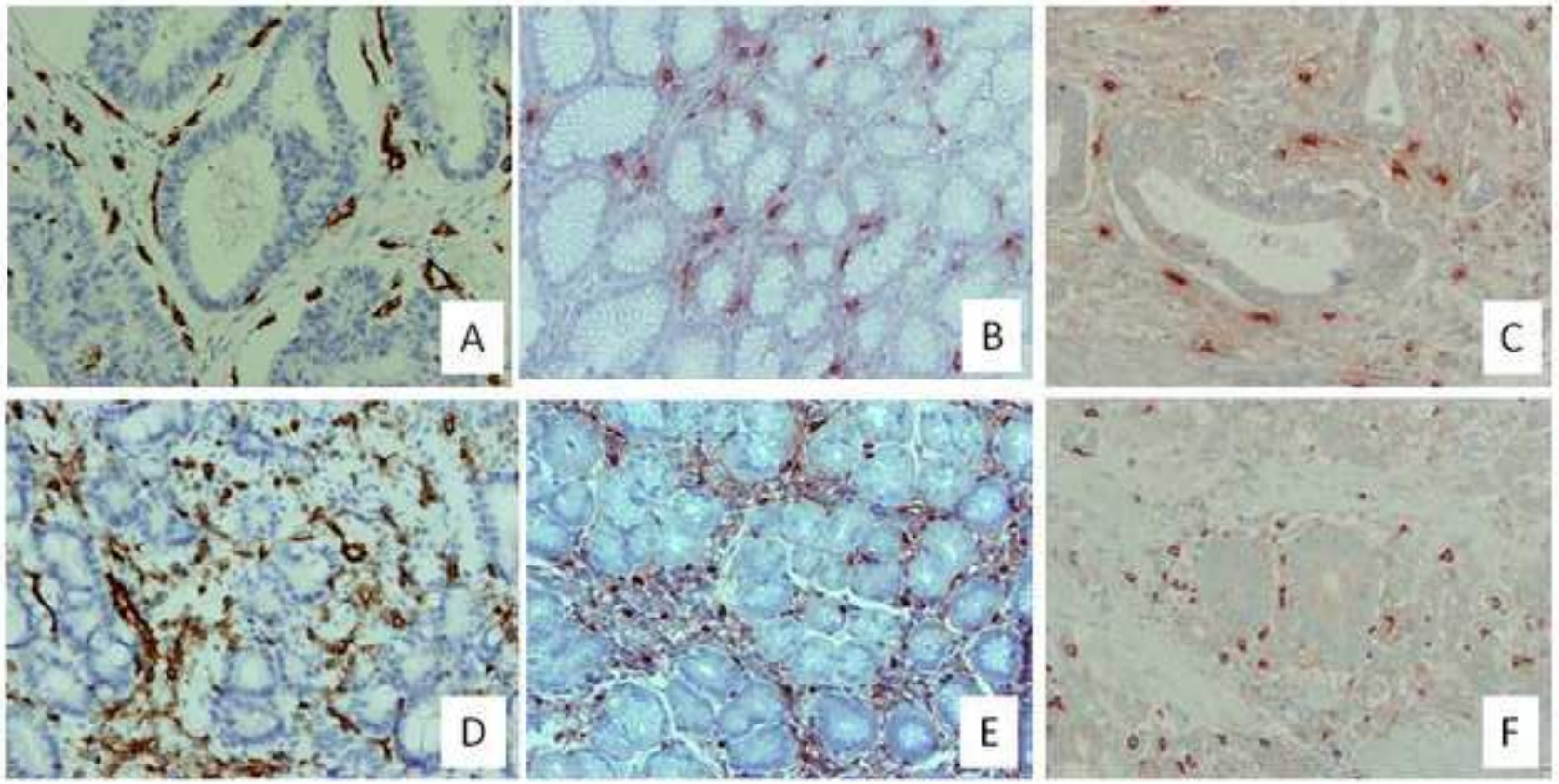

Figure 5

Click here to download Figure Fig5.jpg

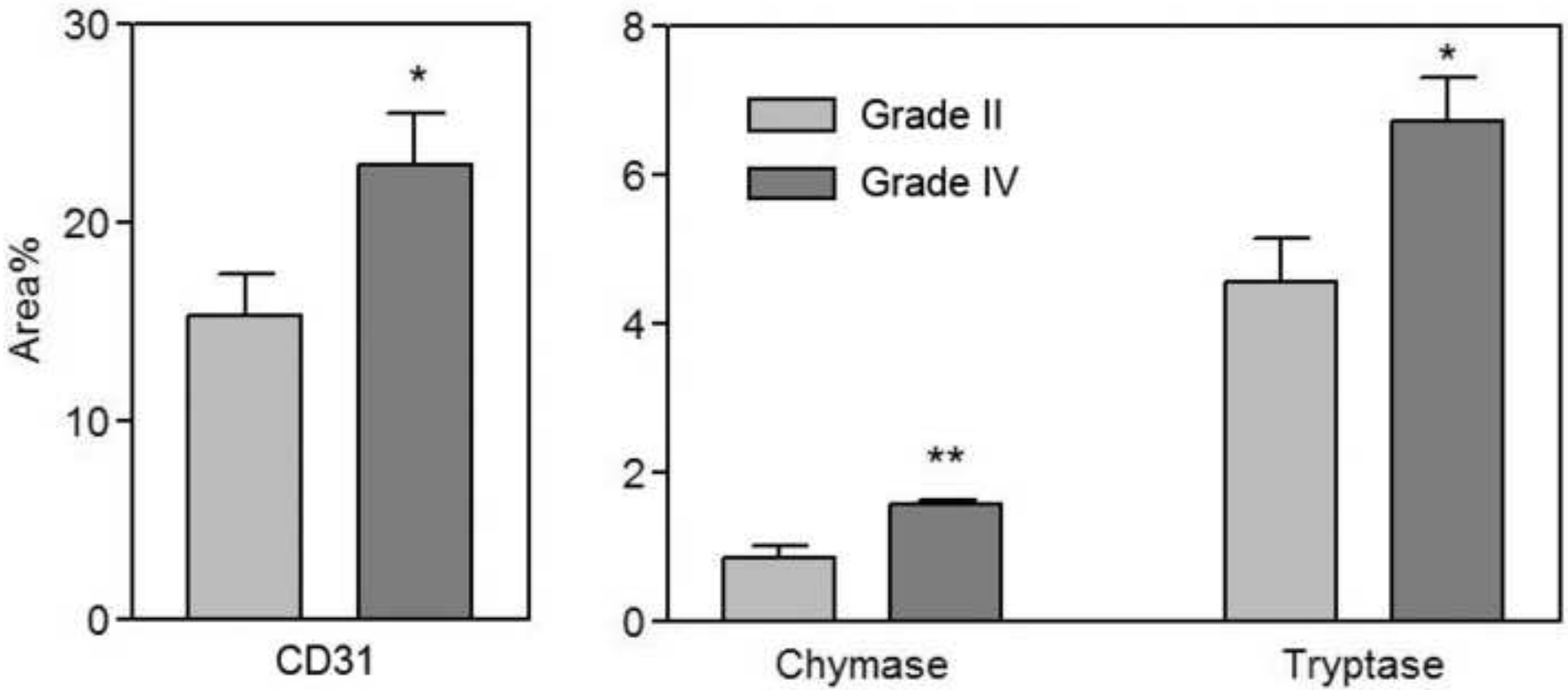

Figure 6

Click here to download Figure Fig6.jpg

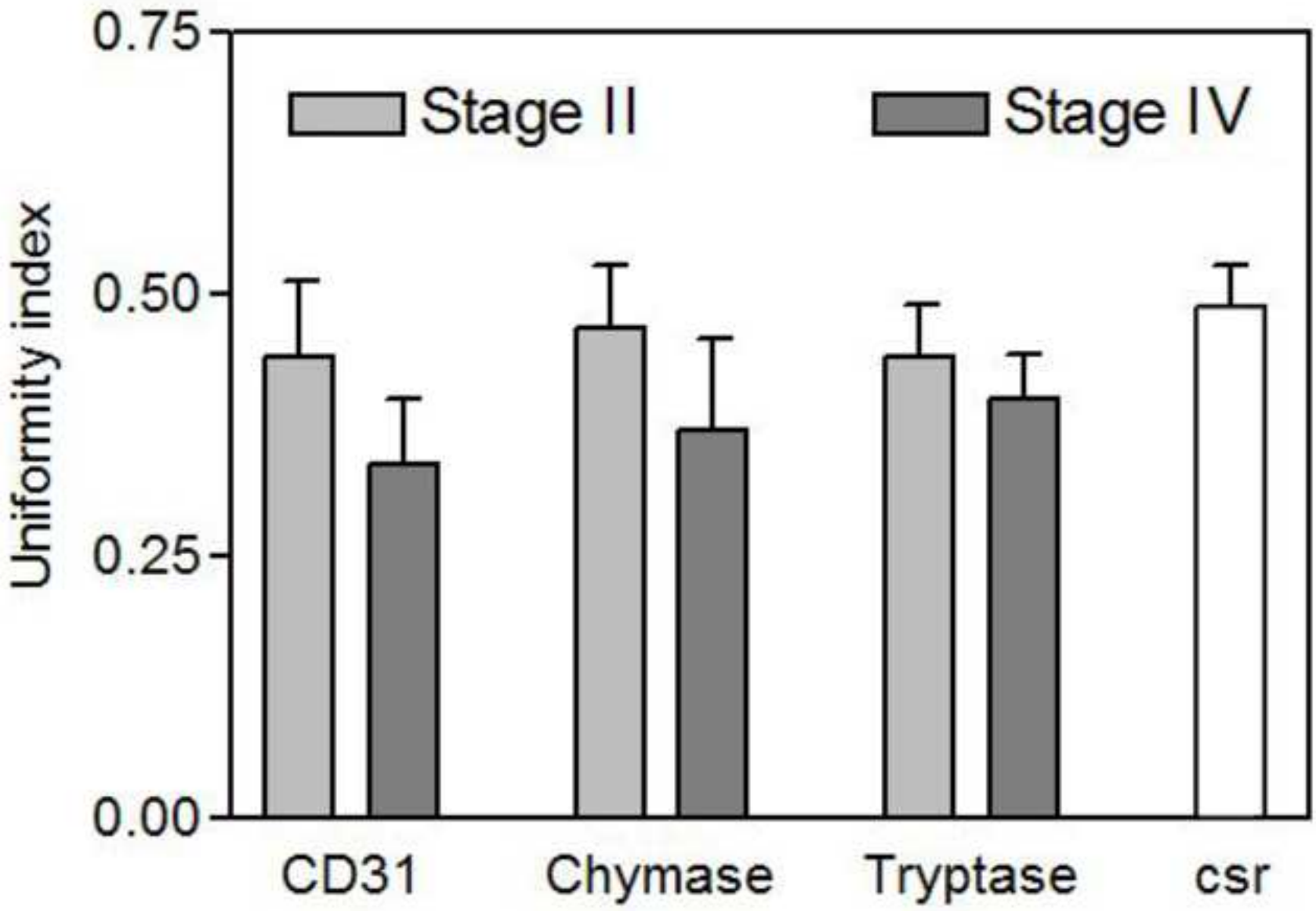

Figure 7

Click here to download Figure Fig7.jpg